Phytopathology® • 2022 • 112:2296-2309 • https://doi.org/10.1094/PHYTO-03-22-0105-R

Bacteriology

Xylella fastidiosa Outbreak in Israel: Population Genetics, Host Range, and Temporal and Spatial Distribution Analysis

Noa Zecharia,[1,2] Helena Krasnov,[1] Miri Vanunu,[1,2] Andreina Castillo Siri,[3] Ami Haberman,[4] Orit Dror,[1] Lera Vakal,[1] Rodrigo P. P. Almeida,[3] Lior Blank,[1] Dani Shtienberg,[1] and Ofir Bahar[1,†]

[1] Department of Plant Pathology and Weed Research, Agricultural Research Organization, Volcani Institute, Rishon LeZion, Israel
[2] The Robert H. Smith Faculty of Agriculture, Food and Environment, The Hebrew University of Jerusalem, Rehovot, Israel
[3] Department of Environmental Science, Policy and Management, University of California, Berkeley, CA, U.S.A.
[4] The Plant Protection and Inspection Services, Ministry of Agriculture and Rural Development, Rishon LeZion, Israel
Accepted for publication 29 June 2022.

Abstract

Diseases caused by the insect-transmitted bacterium *Xylella fastidiosa* have been reported in the Americas since the 19th century, causing diseases such as Pierce's disease of grapevine, almond leaf scorch (ALS), and citrus variegated chlorosis. In the last decade *X. fastidiosa* was reported from different parts of the world, most notably from southern Italy, infecting olives. In 2017, *X. fastidiosa* was reported to be associated with ALS symptoms in Israel. Here, we investigated the causal agent of ALS in Israel, its genetic diversity, and host range, and we characterized the temporal and spatial distribution of the disease. *X. fastidiosa* subsp. *fastidiosa* sequence type 1 was isolated from symptomatic almond trees and was used to infect almond and grapevine by mechanical inoculation. The pathogen, however, did not infect olive, peach, cherry, plum, nectarine, clementine, and grapefruit plants. Genomic analysis of local isolates revealed that the local population is derived from a single introduction and that they are closely related to *X. fastidiosa* strains from grapevines in California. Distribution analyses revealed that ALS did not expand from 2017 to 2019; however, since 2020, newly symptomatic trees appeared in the tested orchards. Symptomatic trees were located primarily in clusters, and symptoms tended to spread within rows. Our study confirms that *X. fastidiosa* is the causal agent of ALS in Israel and describes its genetic and host range characteristics. Although there is no clear evidence yet for the identity of the vectors in Israel, ALS spread continues to threat the almond and grapevine industries in Israel.

Keywords: bacterial pathogens, epidemiology, genomics

Xylella fastidiosa is an insect-transmitted bacterium that infects a wide range of host plants (Delbianco et al. 2021; Hill and Purcell 1997). Insect vectors acquire *X. fastidiosa* by feeding on the xylem sap of infected plants and afterward infect plants by delivering the bacterium to their xylem vessels (Purcell and Finlay 1979). In compatible hosts, *X. fastidiosa* cells multiply in and spread throughout the plant vascular system, leading to desiccation of leaves and branches and even plant death (Hopkins 1989; Saponari et al. 2013). Desiccation and scorching symptoms develop as xylem vessels are being clogged by both pathogen multiplication and aggregation, and tyloses formed by the plant in an attempt to block bacterial spread (Sun et al. 2013). In line with its fastidious growth characteristic, disease symptoms resulting from *X. fastidiosa* infection can take months or even years to express (Bragard et al. 2019; Janse and Obradovic 2010; Saponari et al. 2017).

†Corresponding author: O. Bahar; ofirb@agri.gov.il

Funding: This work was supported by the Chief Scientist of the Ministry of Agriculture and Rural Development of Israel and the Fruit Council (grant 20-02-0115), the European Union Horizon 2020 Research and Innovation Programme under grant agreement 635646 (Pest Organisms Threatening Europe), and the PD/GWSS Research Program at the California Department of Food and Agriculture and the European Union Horizon 2020 Research and Innovation Programme under grant agreement 727987: "*Xylella fastidiosa* Active Containment Through a Multidisciplinary-Oriented Research Strategy XF-ACTORS."

***e*-Xtra:** Supplementary material is available online.

The author(s) declare no conflict of interest.

Reports of *X. fastidiosa* as a disease agent date back to the late 19th century in California vineyards, causing what is known today as Pierce's disease of grapevines (PD) (Pierce 1892). Today, most southern areas of the United States where grapes are grown have documented PD, and the damage caused by *X. fastidiosa* to the California grape industry alone was recently estimated to be $104 million per year (Tumber et al. 2014). *X. fastidiosa* is also the causal agent of citrus variegated chlorosis in Brazil (Chang et al. 1993) and of almond leaf scorch (ALS) and oleander leaf scorch in California (Davis et al. 1980; Purcell et al. 1999).

The species *X. fastidiosa* has been classified into three major subspecies that have diversified in allopatry (Nunney et al. 2012, 2014a, 2014b; Scally et al. 2005). Subspecies *multiplex*, *fastidiosa*, and *pauca* are proposed to have evolved in North, Central, and South America, respectively. Multilocus sequence typing (MLST) has been commonly used to classify *X. fastidiosa* isolates to different sequence types (STs) based on the nucleotide sequence of seven housekeeping gene alleles (Scally et al. 2005). Although MLST is still used, this tool has been shown to have drawbacks when compared with utilization of whole genome sequence data for the purpose of understanding pathogen dispersal and introductions that have led to new outbreaks. Sequence types assigned with MLST might not be monophyletic (Landa et al. 2020), and there is substantial within-ST diversity that is necessarily ignored when isolates are collapsed at that taxonomic level (Castillo et al. 2021; Vanhove et al. 2020). The phylogenetic placement of isolates is of importance because *X. fastidiosa*, as a species, has a very wide host plant range that includes over 600 plant species (Delbianco et al. 2021), but the host range of a particular ST or phylogenetic clade can be rather narrow (Sicard et al. 2018). Therefore, the risk assessment of *X. fastidiosa* introductions, as well as the selection and implementation of quarantine and containment strategies, relies on the phylogenetic placement of isolates.

X. fastidiosa was not detected outside of the Americas for over a century since its first description (Purcell and Hopkins 2002), and although *X. fastidiosa* infections were reported in Taiwan (Leu and Su 1993; Su et al. 2013) and Iran (Amanifar et al. 2009), no major outbreaks were reported outside the Americas. This dramatically changed in 2013 when *X. fastidiosa* was first identified in Europe, infecting ancient olive trees in southern Italy and causing olive quick decline syndrome (Saponari et al. 2013). MLST analysis showed that the sole *X. fastidiosa* genotype in olives in southern Italy is *X. fastidiosa* subsp. *pauca* ST53 (Loconsole et al. 2016), which originated from Central America (Sicard et al. 2021) and is transmitted in this region primarily by the meadow spittlebug *Philaenus spumarius* L. (Hemiptera: Aphrophoridae) (Cornara et al. 2016). The disease in Italy spread rapidly and now covers over 715,000 ha, threatening approximately 21 million olive trees (Martelli et al. 2015; Saponari et al. 2017, 2019). The effect of the *X. fastidiosa* epidemic has been devastating to the olive industry in southern Italy and to its landscape (Cornara et al. 2017; Saponari et al. 2019). A recent study in the European Union estimates future losses to the olive industry in Italy of up to €5.2 billion over 50 years (Schneider et al. 2020).

Not long after its discovery in Italy, *X. fastidiosa* was also reported in other European countries, including France (mainland and the island of Corsica) (Denancé et al. 2017; EFSA 2015, 2018), Spain (mainland and Balearic islands) (Olmo et al. 2017), and Portugal (Delbianco et al. 2021), infecting different crop plants and ornamentals (Bragard et al. 2019; Jacques et al. 2016; Olmo et al. 2017). In Spain, multiple *X. fastidiosa* subspecies and STs were found infecting cherry, almonds, grapevines, and other species (Bragard et al. 2019; Giampetruzzi et al. 2019; Landa et al. 2020; Moralejo et al. 2019; Olmo et al. 2017). Whereas these reports have only appeared in the last 6 years, recent studies suggest that *X. fastidiosa* was introduced into different European countries 20 or more years ago (Moralejo et al. 2020; Soubeyrand et al. 2018). Hence, although being reported in the Mediterranean basin recently, *X. fastidiosa* was probably in this area for much longer and could have been established in additional countries in the region that have not yet identified or reported its presence.

Following the reports from Italy, routine surveys for *X. fastidiosa* were conducted in Israel by the Plant Protection and Inspection Services (PPIS) in olive, grapevine, and almond orchards. During the summer of 2017, almond trees from northern Israel, showing leaf scorching symptoms, were tested and found to be infected with *X. fastidiosa*. A survey conducted by the PPIS in 2018 to map ALS disease in Israel found that the epicenter of the disease was in the Hula Valley in northern Israel. A few orchards with infected trees were also found south of the Hula Valley, but no infection was found in the central or southern regions of Israel, although almonds are also grown in these regions (https://gd.eppo.int/reporting/article-6551; Fig. 1). Almond orchards are intensively farmed in Israel using modern irrigation systems and mechanical harvesting. Locally bred cultivars such as Um El Fahem (UEF, approximately 70% of the trees) and its pollinizers (cultivars Kochav, Gilad, Shefa, and Kochba) are the main almond cultivars in Israel. Over the past few years, almond orchard planting has expanded from 4,500 to 6,200 ha, yielding 6,000 tons annually. The discovery of *X. fastidiosa* and ALS in Israel provoked significant concerns among almond producers and farmers growing other *X. fastidiosa*-susceptible hosts such as grapes, olive, and citrus, as well as regulatory agencies and policy makers.

The goal of this work was to study the biology of *X. fastidiosa* and the epidemiology of ALS disease in Israel. Specifically, the objectives were (i) to identify the causal agent of the leaf scorching symptoms in almond trees, (ii) to examine the genetic diversity of local *X. fastidiosa* isolates, (iii) to determine the host range of local *X. fastidiosa* isolates, and (iv) to characterize the temporal and spatial distribution of ALS disease within infected orchards.

Materials and Methods

The causal agent of the leaf scorching symptoms in almond trees

Bacterial isolation from plant material and *X. fastidiosa* identification. To isolate *X. fastidiosa* from infected plant tissue, 500 mg of leaves and petioles showing ALS symptoms were washed thoroughly in mild soap and water, cut into small pieces with a sterile razor blade, and surface-disinfected using 2% sodium hypochlorite and 70% ethanol (2-min wash in each solution), then rinsed three times with sterile distilled water. The disinfected samples were homogenized in Bioreba extraction bags using the semiautomated homogenizer Homex 6 (Bioreba, Switzerland) with 5 ml of phosphate buffered saline (PBS) buffer (pH 7.4). Extract aliquots (1 ml) were transferred into a 1.7-ml Eppendorf tube, and a series of 10-fold dilutions was performed. Six separated drops of 10 µl from each dilution were spotted on PD3 agar plates (Davis et al. 1981) containing 40 mg/liter of cycloheximide and incubated at 28°C for 1 to 3 weeks. Colonies suspected as *X. fastidiosa* were scraped and resuspended in PBS, tested by PCR (as described below), and, if positive, re-plated on PD3 plates and grown for ~2 weeks before being resuspended with 50% glycerol and stored at −80°C.

DNA extraction from plants and bacterial cultures. To purify DNA from plant samples, we used a modified cetyltrimethylammonium bromide (CTAB) procedure (Zhang et al. 1998). Five hundred milligrams of leaf and petiole tissue were homogenized

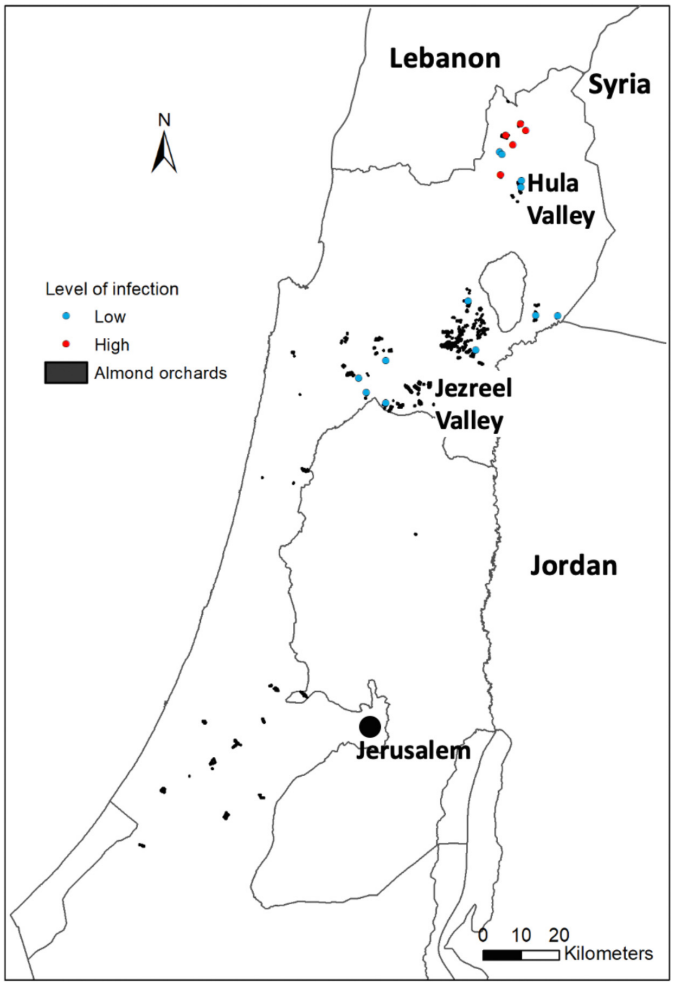

Fig. 1. Almond leaf scorch (ALS) incidence map in Israel. Black dots represent areas where almonds are commercially grown, red dots indicate orchards with significant ALS incidence (more than 1% incidence), and blue dots represents orchards with sporadic incidence of ALS (few isolated symptomatic trees). The locations of Hula Valley and Jezreel Valley are indicated.

in extraction bags using the semiautomated homogenizer Homex 6 (Bioreba) with 5 ml of CTAB buffer and 10 µl of 1M dithiothreitol. Extract aliquots (1.5 ml) were transferred into a 2-ml Eppendorf tube and incubated at 65°C for 45 min with occasional mixing by vortex. The DNA extraction procedure continued as previously described (Mawassi et al. 2018). DNA purity and concentration were evaluated using a NanoDrop device (Thermo Scientific, U.S.A.). DNA purification from *X. fastidiosa* cultures was done by scrapping 2-week-old colonies from PD3 plates and resuspending in PBS. Resuspended cells were then harvested by centrifugation at 9,500 × *g* for 5 min, and the supernatant was discarded. Bacterial DNA was purified from cell pellets using the Macherey-Nagel NucleoSpin Microbial DNA kit ((Düren, Germany; based on silica membrane technology) according to the manufacturer's instructions.

Conventional and quantitative PCR (qPCR). Conventional PCR was performed using 20 ng of template DNA and the DreamTaq Green PCR Master Mix (Thermo Scientific) as previously described (Minsavage et al. 1994; Scally et al. 2005). The RST31/RST33 primers (Minsavage et al. 1994) were used for *X. fastidiosa* initial identification, and the MLST primers (Scally et al. 2005) were used to determine the *X. fastidiosa* sequence type. For MLST analysis, 20 µl of the PCR reaction was used to purify and sequence the PCR product by Sanger sequencing at HyLab laboratories (Israel). Quantitative-PCR (qPCR) was performed using 20 ng of template DNA in duplicates, using the TaqMan Fast Advanced Master Mix (Thermo Scientific) according to Harper et al. (2010). Samples were designated positive (cycle threshold [Ct] < 33), marginally positive (33 < Ct < 36), or negative (Ct = ND, or >36).

Genetic diversity of local *X. fastidiosa* isolates

***X. fastidiosa* whole genome sequencing, assembly, and annotation.** Seven *X. fastidiosa* strains isolated from different almond orchards in Israel (Supplementary Table S1) were selected for whole genome sequencing and downstream analyses. Bacterial DNA was purified as describe above and sequenced using Illumina (HiSeq2000 at the University of California, Berkeley, Vincent J. Coates genomics sequencing laboratory; California Institute for Quantitative Biosciences). All raw reads and information regarding each strain have been submitted to the following bioproject: PRJNA817832. The quality of raw paired FASTQ reads was evaluated using FastQC (Andrews et al. 2018). Low-quality reads and adapter sequences were removed from all paired raw reads using seqtk v1.2 (https://github.com/lh3/seqtk) and cutadapt v1.14 (Marcel 2011) with default parameters. After preprocessing, strains were assembled de novo with SPAdes v3.13 (Bankevich 2012; Nurk et al. 2013) using the *-careful* parameter and -k of 21, 33, 55, and 77. Assembled contigs were reordered using Mauve's contig mover function (Rissman et al. 2009) with the complete publicly available Temecula1 assembly (GCA_000007245.1) as the reference. Assembled and reordered genomes were then individually annotated using the Prokka pipeline (Seemann 2014).

A close evaluation of isolate SN17-2, BL19-1, and HY19-1 assemblies and annotation suggested potential contamination. Contaminant sequences were filtered by mapping FASTQ reads against the RO19-1 assembly using bowtie2 v2.3.4.1 (Langmead and Salzberg 2012) without the *-unal* parameter. Strain RO19-1 was chosen for this task because its phylogenetic relation with the three strains was similar (see later methods for phylogenetic tree construction). Briefly, Samtools v1.8 (Li et al. 2009) was used with the *-f 2* flag to create a BAM file of reads mapped in the proper pair order. Then, the BAM file was sorted by read name using the *-n* flag. Finally, Bedtools v2.26.0 (Quinlan and Hall 2010) was used to convert the sorted BAM file into filtered FASTQ files. The filtered files were assembled using SPAdes v3.13 as previously described. Unfortunately, the number of remaining FASTQ reads for isolate BL19-1 was limited, resulting in low-quality assembly and annotation. Later phylogenetic analyses showed that this strain clustered with divergent groups, suggesting remaining assembly issues. For this reason, BL19-1 was removed from subsequent analyses in the manuscript. Assembly statistics for all remaining newly sequenced isolates can be found in Supplementary Table S1.

Core genome alignments and construction of maximum likelihood trees with and without recombination. Roary v3.11.2 (Page et al. 2015) was used to generate a core genome alignment between grapevine-infecting subsp. *fastidiosa* strains and the newly sequenced Israel strains (1,706 core genes). Three isolates from Costa Rica (non-grapevine infecting) were used to root the tree. The core genome alignment was used to build a maximum likelihood (ML) tree with RAxML (Stamatakis 2014). The GTRCAT substitution model was used on tree construction, and tree topology and branch support were assessed with 1,000 bootstrap replicates. A second smaller core genome alignment (1,686 core genes) and ML tree were constructed for strains clustering in the same clade as the Israeli strains. The same Costa Rican isolates were used to root the tree. In both instances, the core genome alignments were used to estimate the frequency and location of recombinant events. FastGEAR (Mostowy et al. 2017) was used with default parameters to identify lineage-specific recombinant segments (ancestral) and strain-specific recombinant segments (recent). It should be noted that fastGEAR was designed to test recombination in individual gene alignments instead of core genome alignments; however, previous studies have found that recombination detection with fastGEAR is more conservative than with other more appropriate recombination detection methods (Vanhove et al. 2020). Subsequently, all recombinant events were removed from the entire alignment to generate non-recombinant core genome alignments and non-recombinant ML trees. The non-recombinant core alignment was realigned using MAFFT with default parameters (Katoh and Standley 2013). The non-recombinant trees were built with RAxML as previously described.

Population genomics analyses. Global measures of genetic diversity were estimated using the R package 'PopGenome' (Pfeifer et al. 2014). A core genome alignment of exclusively grapevine-infecting isolates (i.e., no Costa Rican isolates) was generated using Roary v3.11.2. The dataset (1,826 core genes) was divided by the geographic origin of the isolates: California, United States ($n = 140$); Southeast United States ($n = 31$); Spain ($n = 2$); Taiwan ($n = 33$); and Israel ($n = 6$). Then, the number of single nucleotide polymorphisms (SNPs), nucleotide diversity (π), Tajima's D (Tajima 1989), and the Watterson's estimator (θ) (Watterson 1975) were computed for the entire alignment. Nucleotide diversity (π) measures the average number of nucleotide differences per site in pairwise comparisons among DNA sequences. Tajima's D calculates the amount of polymorphism present in a population and compares that value to the expectation under neutrality. The Watterson θ estimator measures the mutation rate of a population. All analyses were performed using the core genome alignment and then repeated using the core genome alignment with removed recombinant segments (non-recombinant core). The non-recombinant core was generated as previously described.

Host range of local *X. fastidiosa* isolates

***X. fastidiosa* inoculum preparation, plant inoculations, and assessment of *X. fastidiosa* migration in planta.** Four locally isolated strains of *X. fastidiosa* (SN17-1, SN17-2, SN17-4, HY19-1) were used for inoculation studies. A reference *X. fastidiosa* strain could not be used due to quarantine restrictions. *X. fastidiosa* strains were streaked from glycerol stocks onto PD3 plates and incubated at 28°C for 2 weeks. The inoculum was prepared by scraping *X. fastidiosa* colonies from PD3 plates and resuspending them in PBS, adjusting OD_{600} to ~0.80, corresponding to approximately 10^8 CFU/ml. Pathogenicity tests were performed with 1- to 2-year-old plantlets of *Prunus dulcis* (almond, cultivars UEF and Matan,

grafted on GF677 rootstocks), *Vitis vinifera* (wine grapes, cultivars Shiraz, Carignan, and French Colombard, and table grapes, cultivars Autumn Royal and Big Pearl), *Prunus persica* (peach, cultivar Sugar May grafted on GF677), *Prunus* subg. *Prunus* (plum, cultivar Ogdan grafted on GF677), *Prunus persica* (nectarine, cultivar N/A), *Olea europaea* (olive, cultivars Souri and Barnea), *Prunus avium* (cherry, cultivar Burla), and *Citrus* × *reticulata* and *Citrus* × *paradisi* (cultivars Orri and Star Ruby, respectively). Trees were grown in 8-liter pots containing commercial potting media and were drip-irrigated daily with a fertilized solution. Trees were grown inside a screen house (50 mesh) with no temperature control and exposed to natural light. For each crop species, a minimum of eight trees were used, as described in Table 2, including at least three plants serving as controls. Inoculation was conducted by placing a 10-µl inoculum drop on a green shoot near a petiole and then pricking the stem through the drop five times with a sterile needle (25G). In each tree, two shoots were inoculated. Negative control trees were inoculated similarly with a 10-µl drop of sterile PBS (pH 7.4). Tree inoculations were repeated three times, in April, June, and early September 2019, and were done on the same shoots. In the subsequent year, crop trees that did not display disease symptoms were reinoculated as described in 2019, in early May, late May, and mid-June. Disease symptom development was monitored from 2 weeks postinoculation every 7 to 10 days. Under our screen house conditions, the deciduous species (*Prunus* and *Vitis* species) started senescing during late December, allowing us to assess *X. fastidiosa* symptoms during October and November (2019). *X. fastidiosa* was re-isolated from a subset of symptomatic almond and grapevine plants (five or more for each crop), and colonies were examined by PCR with *X. fastidiosa*-specific primers, as described above. To estimate the virulence of local *X. fastidiosa* on the tested crops, the incidence of disease symptoms in each plant was evaluated by counting the number of symptomatic and asymptomatic leaves in each inoculated shoot and calculating the percentage of symptomatic leaves. To assess *X. fastidiosa* establishment at the inoculation point (IP) and above, inoculated shoots were removed, and stem and petiole tissue were sampled from the IP and from further above the IP (20 cm above the IP in symptomatic trees and 5 cm above the IP in asymptomatic trees) 2 months after the final inoculation. The presence and relative population of *X. fastidiosa* were determined in two branches per plant by qPCR, as described above. A generalized linear model with binomial distribution and logit function was fitted to the data to analyze symptom incidence on different crop plants. Analysis of variance (ANOVA) was used to compare qPCR Ct values at the IP and above. When appropriate, ANOVA was followed by a post-hoc Tukey-Kramer HSD test for multiple means comparison. Differences in *X. fastidiosa* incidence at the IP or above among different crops were tested by the Pearson χ^2 test.

The temporal and spatial distribution of ALS disease within infected orchards

To better study the spatial and temporal spread of ALS in Israel, we selected orchards from Hula Valley and Jezreel Valley, representing orchards with high and low ALS incidence (Fig. 1), respectively, and monitored ALS appearance over time. In Hula Valley, the monitoring was conducted in two almond orchards (orchard 1; 33°11′45.2″N 35°37′48.8″E; and orchard 2, 33°09′02.3″N 35°36′46.3″E) located ~5 km apart. Both orchards were planted during 2006 to to 2007, drip irrigated, and subjected to conventional almond-growing practices including disease and pest control with authorized chemicals. One subplot was monitored in each orchard: subplot 3 in orchard 1 and subplot 1 in orchard 2. These subplots will be referred to hereafter as subplots 1-3 and 2-1, respectively. Each subplot consisted of approximately 1,100 trees of several cultivars grafted on GF677 rootstock; the predominant cultivar in both orchards was UEF, which accounted for two-thirds of the trees in the orchard. Other cultivars, serving as pollinators, were 'Kochba', 'Kochav', and 'Shefa' in orchard 1 and 'Shefa', 'Kochba', and 'Napa' in orchard 2. In both plots, a similar cultivar-planting template was used, in which there were two rows of the main cultivar UEF followed by a row of one of the pollinator cultivars. The distance between two trees within the same row was 6 m, and between rows was 7 m. Starting in 2017, every summer (July through August), for five consecutive years (2017 to 2021), each tree in the two selected subplots was examined visually, and the severity of ALS symptoms was recorded using the following scale: 1, no symptoms; 2, up to 50% of the canopy display ALS symptoms; 3, more than 50% of the canopy display ALS symptoms; and 4, dead or uprooted tree. In Jezreel Valley, due to the scarcity of ALS symptoms, monitoring was performed differently than above. Here, 11 symptomatic almond trees positive for *X. fastidiosa* and surrounded by asymptomatic trees were selected from five different orchards, and the appearance of new symptomatic trees was monitored in a square of 7 × 7 trees around the symptomatic tree. The ALS severity scale described above was used here as well. Monitoring was done for three consecutive years (2017 to 2019). To analyze the spatial pattern of ALS in the infected orchards, we further used a GPS-based dataset generated in 2018, in which the exact coordinates of each tree with ALS symptoms in the two orchards described above (orchard 1 and 2 in Hula Valley) were collected. This dataset included all subplots in orchard 1 (nine subplots) and orchard 2 (six subplots). Subplots are separated from one another by a gravel road approximately 4 m wide.

The spatial pattern of ALS trees in Hula Valley was tested with two questions in mind: (i) Are the symptomatic trees aggregated or randomly dispersed? (ii) Does ALS progress within the infected orchard omnidirectional or is it progressing in a particular direction? To determine whether symptomatic trees were aggregated, we used Ripley's k-function (Ripley 1976) for spatial autocorrelation, where each tree received a value of $K(r)$ representing the number of neighboring symptomatic trees in a radius r. Ripley's K allowed us to determine if the symptomatic trees appeared to be dispersed, clustered, or randomly distributed throughout the study area (Ben-Hamo et al. 2020).

$$K(r) = \frac{a}{n(n-1)} \cdot \sum_{i,j} I\left(d_{i,j} \le r\right) \cdot e_{i,j}$$

where a is the area of the sampled block of trees, n is the number of symptomatic trees in the block, and I receives a value of 0 or 1 to denote the presence of symptomatic trees within radius d of the focal tree. Radius d is defined to be equal to or smaller than radius r. Finally, e is a function correcting for the outer limits of the tree block. We then compared our calculated value of K to a theoretical estimate of K, which assumes a random distribution of symptomatic trees within each block. A calculated value of K higher than the theoretical estimate is indicative of clusters of symptomatic trees.

To determine the direction of ALS progression, we constructed a logistic regression model in which we assessed how trees in the orchards are affected by symptomatic neighboring trees within the same row, or in adjacent rows (Sparks et al. 2008), using the following equation:

$$\widehat{Z}_t(x) = \frac{1}{2} \cdot \left(Z_t(x-1) + Z_t(x+1)\right)$$

where x denotes the location of the tree in the orchard, t is the time at which the plot was surveyed, and z denotes the presence of symptoms in a particular tree in the orchard (Ben-Hamo et al. 2020). The presence of symptoms was determined as describe above, with any tree receiving a severity score higher than 1. The model that best describe the spatial progression of ALS was determined by a combination of the P and AIC values. As the number of symptomatic trees in both subplots remained stable from 2017 to 2019, we analyzed the first 3 years together. The year was added as a random

effect but was not statistically significant, meaning there were no differences between years. In 2020 and 2021, the analysis was done for each year separately because the number of symptomatic trees increased. This analysis was done using the R package 'spatstat' (Baddeley et al. 2015).

Results

The causal agent of the leaf scorching symptoms in almond trees

ALS symptoms were typically visible in almond trees from early June and became more pronounced in summer months (July and August). Symptomatic leaves displayed a typical tricolor pattern: scorched leaf tip separated by a golden-yellow strip from the inner (green) part of the leaf (Fig. 2A). Leaf tips were often curled, differentiating ALS from similar symptoms caused by salt and/or other stresses (Fig. 2B). Most symptomatic trees identified in 2017 displayed ALS symptoms on more than 50% of the canopy, justifying the "golden death" term given to severely infected trees (Sanborn et al. 1974) (Fig. 2C). In July 2017, samples were taken from 36 almond trees showing typical ALS symptoms from four different orchards in Hula Valley and tested by qPCR for the presence of *X. fastidiosa*. More than 97% of the tested trees were positive for *X. fastidiosa* (35/36), with a Ct lower than 33. Out of 48 asymptomatic trees sampled, one was marginally positive for *X. fastidiosa* ($33 > Ct > 36$), whereas the rest of the asymptomatic trees were negative (Ct = ND, or >36). In subsequent years (2018 to 2021), more than 100 tests for trees with typical ALS symptoms were performed by ours and the PPIS's laboratories, most of which yielded a positive qPCR result for *X. fastidiosa* (Bahar and PPIS, *personal communication*).

To isolate the causal agent of ALS, crushed leaf petioles from nine symptomatic almond trees were streaked on PD3 plates. Small, white colonies appeared on plates 14 to 21 days after plating (Supplementary Fig. S1), which tested positive for *X. fastidiosa* by colony PCR (RST31/33 primers) and sequencing of the PCR product.

Genetic diversity of local *X. fastidiosa* isolates

To estimate the genetic diversity of *X. fastidiosa* in Israel, we performed MLST analysis on 27 *X. fastidiosa*-positive samples (isolated strains or DNA purified from infected trees) collected from 10 different orchards, as detailed in Supplementary Table S1. All the tested samples had identical sequences in all seven alleles and matched those of *X. fastidiosa* subsp. *fastidiosa* ST1. To study the phylogenetic relationships of *X. fastidiosa* isolates from Israel with isolates from around the world, we sequenced the genomes of seven isolates originating from almond trees in different geographical locations (Supplementary Table S2; Fig. 1). An initial phylogenetic tree with ~400 *X. fastidiosa* isolates demonstrated that the *X. fastidiosa* population from Israel clustered with isolates obtained from grapevine infections in California (data not shown). To provide useful insights, we limited our analyses to *X. fastidiosa* subsp. *fastidiosa* from that clade alone (i.e., *X. fastidiosa* causing disease in grapevines). This analysis demonstrated that the introduction of *X. fastidiosa* to Israel likely originated from a population from California (Fig. 3).

Population genetics statistics support the hypothesis that *X. fastidiosa* was recently introduced into Israel, as it showed a comparable nucleotide diversity within Israeli isolates (SNPs = 1, $\pi = 3.10 \times 10\text{e-}07$) and with other relatively recent *X. fastidiosa* introductions (Table 1). Moreover, there is a clear drop in genetic diversity between the *X. fastidiosa* population in Israel and its source population in California (SNPs = 496, $\pi = 3.54 \times 10\text{e-}05$). Likewise, the Watterson θ estimate shows that the mutation rate in Israel ($3.38 \times 10\text{e-}07$) is also lower compared with California ($5.57 \times 10\text{e-}05$). Alternatively, the Tajima's *D* value, estimating the genetic diversity of a population, was higher within Israel (−0.612) compared with California (−1.202), indicating a lower population polymorphism in Israel (Table 1). Altogether, available data indicate that a single *X. fastidiosa* introduction into Israel occurred relatively recently.

Host range of local *X. fastidiosa* isolates

To determine the pathogenicity of Israeli *X. fastidiosa* isolates on different crop species, we used the needle-prick inoculation method and evaluated symptom development and bacterial migration from the IP for two consecutive years. Typical PD and ALS symptoms were evident in all inoculated grapevine (wine grape cultivars Shiraz, Carignan, and French Colombard, and table grape cultivars Big Pearl ad Autumn Royal) and almond (cultivars UEF and Matan) cultivars 6 and 8 weeks after the last round of inoculation, respectively (Fig. 4). *X. fastidiosa* colonies were successfully

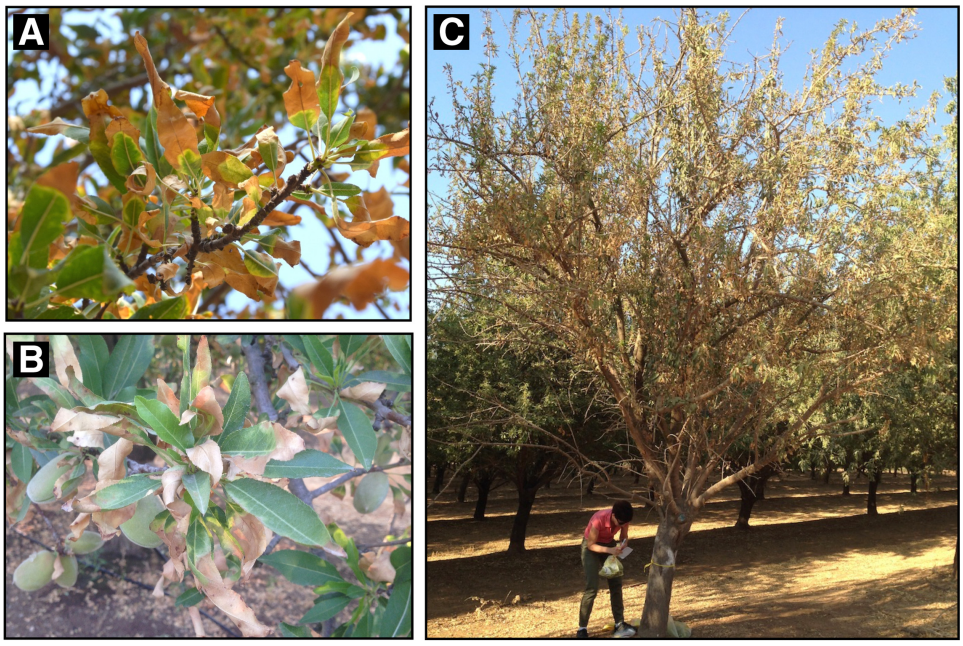

Fig. 2. Almond leaf scorch (ALS) symptoms caused by *Xylella fastidiosa* in Hula Valley. **A,** Symptomatic leaves showing typical tricolor patterns; **B,** scorched leaves showing typical leaf curling; and **C,** *X. fastidiosa*-infected almond tree displaying "golden death," where most of the canopy displays ALS symptoms.

isolated from symptomatic almond and grapevine leaves and confirmed by PCR. All other tested crops (olive, plum, peach, cherry, citrus, and nectarine) did not display disease symptoms (Table 2). In the subsequent year, all crop trees that did not display disease symptoms in the first year were reinoculated, yet none had developed disease symptoms in the second year. Most grapevine and almond cultivars that displayed disease symptoms in the first year and were kept in the screen house with no further inoculation redisplayed PD (14/15) and ALS symptoms (7/9) in the second year (Table 2).

The incidence of PD symptoms among the five grapevine cultivars tested was not statistically different, and similarly, no differences in ALS incidence were seen between the two almond cultivars ($P > 0.05$) (Supplementary Tables S3 and S4; Fig. 5A). Grouping incidence scores from all grapevine cultivars and comparing with almond cultivars revealed that grapevine cultivars were more prone

Fig. 3. Maximum likelihood tree of *Xylella fastidiosa* subsp. *fastidiosa* isolates. Core genomes (1,826 core genes with recombinant regions) of 203 *X. fastidiosa* subsp. *fastidiosa* isolates were used to construct a maximum likelihood tree. The isolates obtained from disease almond trees in Israel (highlighted in light blue or light gray) cluster within a California clade of isolates infecting grapevines.

to develop substantial disease symptoms when infected with the Israeli isolates (average 60.8% symptomatic leaves) than almonds (average 20.6% symptomatic leaves) ($P < 0.05$) (Supplementary Table S5; Fig. 5B).

In addition to disease symptom evaluations, the incidence and relative concentration of *X. fastidiosa* at the IP and further above were also determined. *X. fastidiosa* was detected by qPCR at the IP of nearly all inoculated plants (96/109), regardless of whether they displayed disease symptoms (Table 3). However, ANOVA revealed that the qPCR Ct values obtained were significantly different among the tested crops (one-way ANOVA; $F_{4,82} = 112.43$, $P < 0.001$). A post-hoc Tukey-Kramer HSD test for multiple comparisons showed that the average Ct value of grapevine infections was significantly lower than all other tested crops ($P \leq 0.003$), whereas the average Ct of almonds was significantly lower than that of olive and peach ($P \leq 0.0012$) but not of plum ($P = 0.2814$) (Fig. 5B; Table 3). Citrus and cherry plants were tested in a different year and were therefore not included in this statistical analysis; however, they displayed similar average Ct values to those of crops with no symptoms (Table 3; Fig. 5B). The incidence of *X. fastidiosa* 20 cm above the IP in both almond (11/12) and grapevine plants (15/15) was significantly higher than the incidence of *X. fastidiosa* 5 cm above the IP in plants that did not display disease symptoms ($\chi^2 = 19.951$, df = 3, $P = 0.002$; and $\chi^2 = 26.809$, df = 3, $P < 0.001$, for almonds and grapes, respectively) (Table 3). Here too, the average Ct obtained above the IP was significantly different among the tested crops (one-way ANOVA; $F_{3,29} = 24.80$, $P < 0.001$), and the Tukey-Kramer HSD test revealed that both grapes and almonds had a significantly lower average Ct value ($P < 0.001$) than the other tested crops that did not display disease symptoms (Fig. 5C; Table 3). The average Ct value of *X. fastidiosa* in almonds and grapevines 20 cm above the IP was not significantly different between them ($P = 0.7339$).

The temporal and spatial distribution of ALS disease within infected orchards

To better understand the temporal and spatial dynamics of ALS within orchards in the Hula Valley, we visually monitored trees in two infected subplots from 2017 to 2021 (Fig. 6). In subplot 1-3, there were 39 symptomatic trees (38 with severity level 3) and 5 dead/uprooted trees in 2017, representing 3.51 and 0.46% of the trees, respectively. In the same year, there were 72 symptomatic trees (58 with severity level 3) and 60 uprooted/dead trees in subplot 2-1, representing 6.93 and 5.78% of the trees in the subplot, respectively (Fig. 7). The number of trees affected by *X. fastidiosa* (i.e., trees displaying ALS or trees with ALS that had been uprooted) in these plots remained mostly unchanged from 2017 to 2019, suggesting that there was very little, if any, increase in ALS incidence within the monitored orchards during this time (Figs. 6 and 7). Similarly, the ratios among the different disease categories had also remained quite constant, indicating that the severity of diseased trees had not changed (Fig. 7). In 2020, on the other hand, the number of symptomatic and dead trees in subplots 1-3 and 2-1 increased by 45 and 30%, respectively (Figs. 6 and 7), mainly due to the addition of trees with a severity score of 2, amounting to 62 (5.73%) and 81 (7.80%) of the total trees in the two subplots, respectively. Surprisingly, many of the trees that received an ALS rating of 2 in 2020 were asymptomatic in 2021; however, the total number of trees affected by *X. fastidiosa* in 2021 remained similar to that observed in 2020.

ALS monitoring was also conducted in Jezreel Valley, where the incidence of ALS was significantly lower than in Hula Valley. Here, 11 sporadically distributed and isolated symptomatic and infected trees (i.e., surrounded by asymptomatic trees) were selected, and the trees surrounding the symptomatic tree (48 trees) were monitored for ALS symptoms from 2017 to 2019. Throughout the duration of

TABLE 1. Population diversity statistics within geographic Pierce's disease-causing populations

Population (*N*)	Alignment length	SNPs	Nucleotide diversity (π)	Watterson's θ	Tajima's *D*
With recombination					
California (140)	1,614,872	496	3.54E-05	5.57E-05	−1.202
Southeast U.S.A. (31)		1,048	1.32E-04	1.62E-04	−0.718
Spain (2)		2	1.24E-06	1.24E-06	–
Taiwan (33)		148	1.03E-05	2.48E-05	−2.355
Israel (6)		1	3.10E-07	3.38E-07	−0.612
Without recombination					
California (140)	1,400,994	518	3.94E-05	6.70E-05	−1.361
Southeast U.S.A. (31)		968	1.37E-04	1.73E-04	−0.805
Spain (2)		2	1.43E-06	1.43E-06	–
Taiwan (33)		145	1.15E-05	2.80E-05	−2.370
Israel (6)		0	0	0	0

TABLE 2. Pathogenicity of *Xylella fastidiosa* strains from Israel on different crop plants

Latin name	Crop	Cultivar	Number of symptomatic trees (year 1)[a]	Number of symptomatic trees (year 2)[b]
Prunus dulcis	Almond	Um El Fahem	4/6	3/6
Prunus dulcis	Almond	Matan	5/6	4/6
Olea europaea	Olive	Suri	0/7	0/7
Olea europaea	Olive	Barnea	0/7	0/7
Vitis vinifera	Wine grape	Shiraz	9/9	5/5
Vitis vinifera	Wine grape	Carignan	10/10	5/5
Vitis vinifera	Wine grape	French Colombard	9/10	N/D
Vitis vinifera	Table grape	Autumn Royal	7/8	4/5
Vitis vinifera	Table grape	Big Pearl	8/9	N/D
Prunus subg. *Prunus*	Plum	Ogden	0/8	0/8
Prunus persica	Peach	Sugar May	0/7	0/7
Prunus persica	Nectarine	N/A	0/6	0/6
Prunus avium	Cherry	Burla	0/5	0/5
Citrus × *reticulata*	Clementine	Orri	0/6	0/6
Citrus × *paradisi*	Grapefruit	Star Ruby	0/6	0/6

[a] In each tree, two shoots were inoculated. Trees were considered symptomatic if one or more shoots were showing symptoms.
[b] Crop trees that were asymptomatic in year 1 were reinoculated in year 2. Crop trees that were symptomatic in year 1 (grapes and almonds) were not reinoculated in year 2. N/D, not determined.

this survey, none of the monitored trees displayed ALS symptoms (Supplementary Fig. S2).

To better understand the distribution pattern of ALS in Hula Valley orchards, and the manner in which it progresses, we analyzed the spatial pattern of ALS in orchards 1 and 2. First, we tested if the distribution of symptomatic trees in these plots was aggregated using Ripley's K-function, where the distance of the estimated K-function (solid black line) from the envelope (gray area) indicates the aggregation change with distance, and the dashed red line represents the theoretical K-function (random distribution). This analysis was done using a GPS-based dataset collected during the summer of 2018 and included all the subplots in these orchards (15 in total; Fig. 8). Symptomatic trees in orchard 1 were significantly aggregated in all subplots except subplots 7 and 8. In the significant subplots, aggregation was mostly observed from a radius of 10 m or higher. In orchard 2, symptomatic trees were randomly distributed in subplots 3, 4, and 6 and aggregated in subplots 1, 2, and 5, at a radius of 10, 25, and 10 to 20 m, respectively (Fig. 8). Investigating the spatial progression of the disease in these orchards was done with one subplot from each orchard and applying a logistic regression model. In both subplots, there was no directional progression of the disease from 2017 to 2019 (Supplementary Tables S6 and S9). However, in 2020 and 2021, we found that in subplot 1-3, there was an omnidirectional distribution of symptomatic trees (Supplementary Tables S7 and S8), whereas in subplot 2-1, the model suggested that ALS spread omnidirectionally in 2020 and within rows in 2021 ($\Delta AIC < 2$; Supplementary Tables S10 and S11).

Discussion

X. fastidiosa was first reported in Israel in 2017 infecting almond trees and causing ALS disease. The center of the current *X. fastidiosa* outbreak is in the Hula Valley located in the northeast part of Israel. Although additional infected trees were found south of Hula Valley, these incidences were sparse and sporadic, and Jezreel Valley represented the southern geographical limit of the infected zone (Fig. 1). The nationwide distribution of infected orchards and

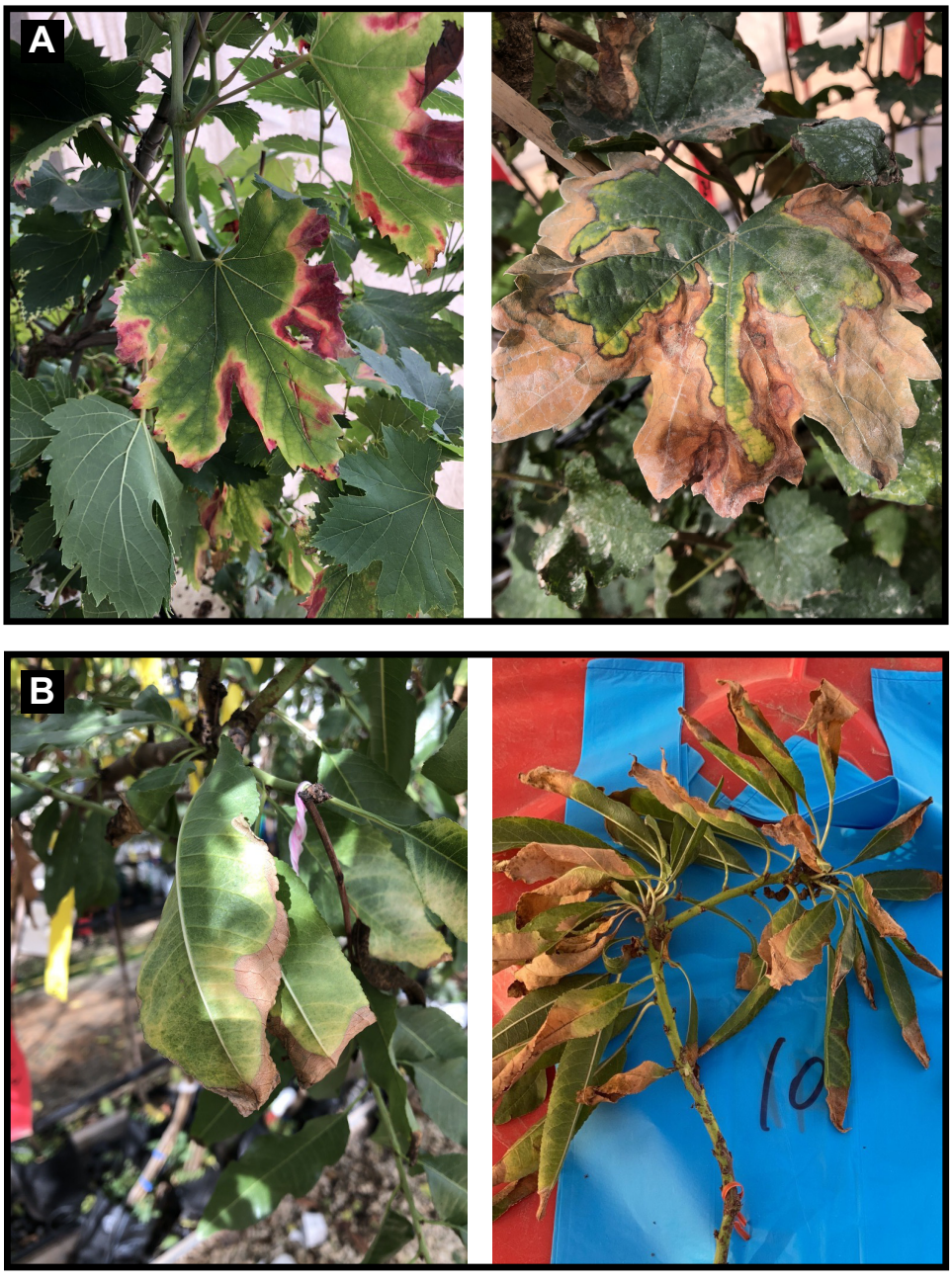

Fig. 4. Pierce's disease (PD) of grapevine and almond leaf scorch (ALS) symptoms following mechanical inoculation. **A,** Grapevine and **B,** almond plants were inoculated with *Xylella fastidiosa* isolates from Israel using the needle-prick inoculation method. Disease symptoms started appearing 6 and 8 weeks postinoculation in grapevine and almond, respectively. Representative images of PD and ALS symptoms from inoculated plants are presented.

the characteristics of the disease in individual trees could be relevant for revealing the origin of the *X. fastidiosa* outbreak in Israel.

Most of the symptomatic trees that were identified during 2017 displayed ALS symptoms on more than 50% of the canopy. The severe ALS expression is indicative of a systemic and substantial infection of the trees, suggesting it had occurred several years before 2017. The fact that we could not find trees at early stages of infection in the following 2 years suggests that there was no significant secondary spread of the pathogen. One possible explanation for this observation is that the symptomatic trees were introduced as infected plantlets from nurseries, and in the absence of a suitable vector to disseminate the disease further, these trees expressed ALS at approximately the same time, and no further infection occurred. This possibility seems unlikely due to several reasons. First, the infected orchards in Hula Valley were all planted during the years 2005 to 2007. Hence, if infected plantlets were the source of initial

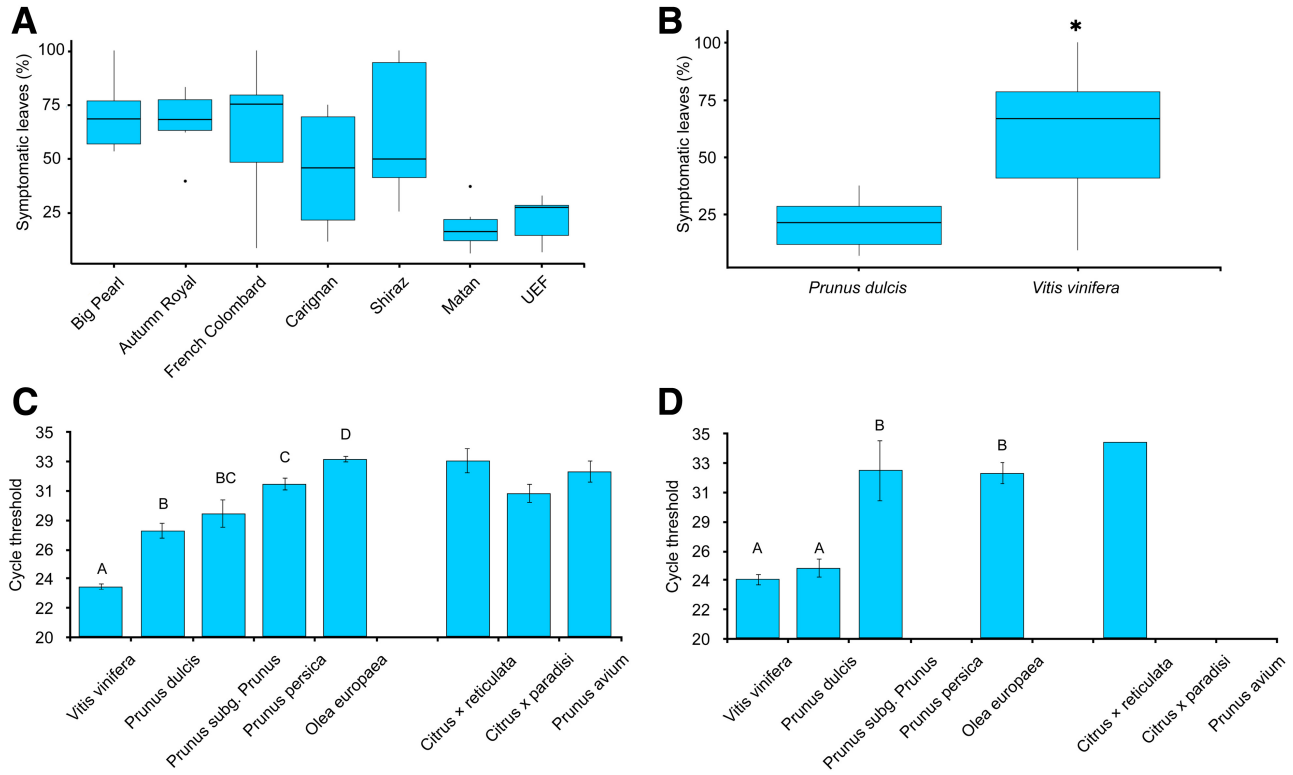

Fig. 5. Symptom incidence in different crop plants mechanically inoculated with *Xylella fastidiosa*. Symptom incidence in different crop plants was evaluated following direct inoculation of plantlets using the needle-prick method. **A,** Symptom incidence was evaluated in November by calculating the percentage of symptomatic leaves in each inoculated branch. **B,** Analysis of symptom incidence grouped by crop. **C,** The incidence and relative concentration of *X. fastidiosa* at the inoculation point (IP) was estimated using qPCR for each tested crop. Lower cycle threshold (Ct) values indicate higher bacterial populations. **D,** *X. fastidiosa* incidence and relative concentration above the IP was evaluated by qPCR. In crops displaying disease symptoms (*Prunus dulcis* and *Vitis vinifera*), the evaluation was done 20 cm above the IP, and in crops that did not develop symptoms (*P.* subg. *prunus*, *P. persica*, *Olea europea*, *Citrus* spp., and *P. avium*), evaluation was done 5 cm above the IP. For each cultivar, 4 to 10 plantlets were used, as detailed in Table 3. In A and B, a generalized linear model with logit function was fitted. Asterisks indicate significant difference ($P < 0.05$) between *V. vinifera* and *P. dulcis* cultivars. In C and D, different letters indicate significant differences ($P < 0.01$) among different crop species, as determined by the Tukey-Kramer HSD test. *Citrus* spp. and *P. avium* were not included in the statistical analysis because they were inoculated in a different year.

TABLE 3. Incidence of *Xylella fastidiosa* and average cycle threshold (Ct) values at the inoculation point and above in different crop plants

			qPCR at the inoculation point		qPCR above the inoculation point[c]	
Latin name	Common name	Cultivar	Positive/tested[a]	Ct ± SD[b]	Positive/tested[a]	Ct ± SD[b]
Prunus dulcis	Almond	Um El Fahem	6/6	27.99 ± 1.42	4/6[a]	24.60 ± 1.09
		Matan	6/6	27.55 ± 2.3	5/6[a]	25.71 ± 2.47
Olea europaea	Olive	Souri	5/7	33.06 ± 1.04	3/7	31.52 ± 1.57
		Barnea	5/7	32.98 ± 0.68	0/7	Undetermined
Vitis vinifera	Wine grape	Shiraz	9/9	23.55 ± 1.44	6/6[a]	25.20 ± 0.36
		Carignan	9/10	25.23 ± 1.06	6/6[a]	26.07 ± 2.27
		French Colombard	10/10	23.19 ± 1.38	6/6[a]	23.81 ± 0.81
	Table grape	Autumn Royal	8/8	23.97 ± 1.42	6/6[a]	23.35 ± 0.29
		Big Pearl	9/9	24.69 ± 3.94	6/6[a]	23.37 ± 0.74
Prunus subg. *Prunus*	Plum	Ogden	8/8	29.07 ± 2.3	2/8	32.31 ± 2.75
Prunus persica	Peach	Sugar May	6/7	31.21 ± 1.44	0/7	Undetermined
	Nectarine	N/A	5/6	31.23 ± 1.99	0/6	Undetermined
Prunus avium	Cherry	Burla	4/4	31.60 ± 1.82	0/4	Undetermined
Citrus × *reticulata*	Clementine	Orri	4/6	32.9 ± 1.83	1/5	34.4
Citrus × *paradisi*	Grapefruit	Star Ruby	2/6	30.5 ± 0.96	0/6	Undetermined

[a] Samples were considered positive for *X. fastidiosa* when Ct values were <33.
[b] Ct averages includes only positive samples.
[c] Samples were collected 5 cm above the inoculation point in asymptomatic plants (olive, plum, peach, nectarine, citrus, and cherry) and 20 cm above the inoculation point in symptomatic plants* (almond, grapes).

inoculum, it is expected that symptoms would have appeared in the years soon after planting, and not 10 years later. Second, there are only a few nurseries in Israel that produce and distribute almond plantlets, and these nurseries distribute their plantlets to all almond-growing regions in the country. Therefore, if the source of infection were nurseries, we would have expected to see symptomatic plants in more almond-growing regions of the country. Third, in this scenario, the source of infection must have been an infected mother tree used for scion collection and plantlets grafting. However, because we observed ALS symptoms in all the cultivars grown in the infected orchards (five cultivars), it is unlikely that the mother trees of all cultivars were infected. Finally, Israel's almond industry is based on local cultivars, and rootstocks are propagated in tissue culture. Therefore, the likelihood of importation of infected almond material into Israel is small. Alternative scenarios include (i) introduction of an infected ornamental plant that served as a source for local vectors to transmit to almonds or (ii) introduction of infected insect vectors that migrated from a neighboring country. However, no ornamental plants have thus far been found to be infected with *X. fastidiosa* in Israel, and the knowledge about possible local vectors is still lacking; hence, the validity of these hypotheses remains to be tested.

Our MLST analysis of multiple *X. fastidiosa* isolates and infected trees indicates that *X. fastidiosa* isolates in Israel belong to a single sequence type, ST1. The genomic data further support the homogeneity of the local *X. fastidiosa* population. Recent studies have shown that nucleotide diversity is larger in native *X. fastidiosa* populations compared with introduced ones (Castillo et al. 2020). This suggests that drops in diversity following introduction events are expected in *X. fastidiosa*. Indeed, the nucleotide diversity among the sequenced *X. fastidiosa* strains was very low and comparable to other locations in the world where *X. fastidiosa* was recently introduced. Additionally, higher Tajima's *D* values indicate lower population polymorphism than expected by neutrality alone; this is often linked to introduction events or selective sweeps (values are affected by sample size). This further supports the notion that the introduction of *X. fastidiosa* into Israel must have been quite recent. It also supports the scenario of a single introduction event;

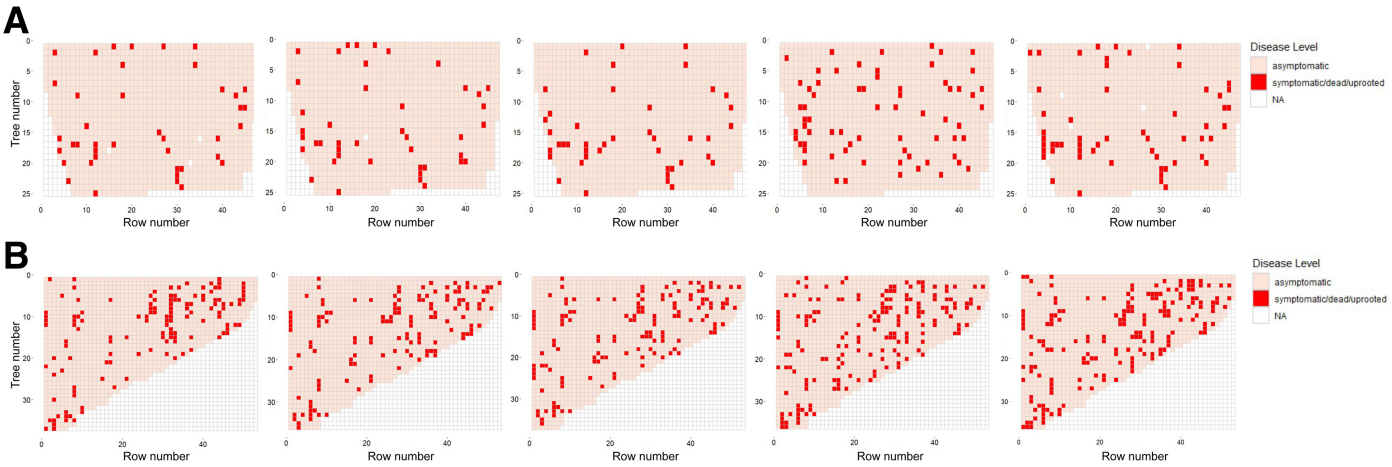

Fig. 6. Long-term monitoring of almond leaf scorch (ALS) in two orchards in Hula Valley. Each tree in **A,** subplot 1-3 and **B,** subplot 2-1 was scored in the summer of every year from 2017 to 2021 for ALS symptoms. In each subfigure, a representation of the status of infected plants in each year is given. Every square in the grid represents a tree, and trees were categorized as symptomatic (trees with disease severity rating of 2 to 4) and healthy (asymptomatic trees, disease severity rating of 0). Blank squares represent parts of the plot where no trees are planted. The *x* axis represents the row number and the *y* axis the tree number.

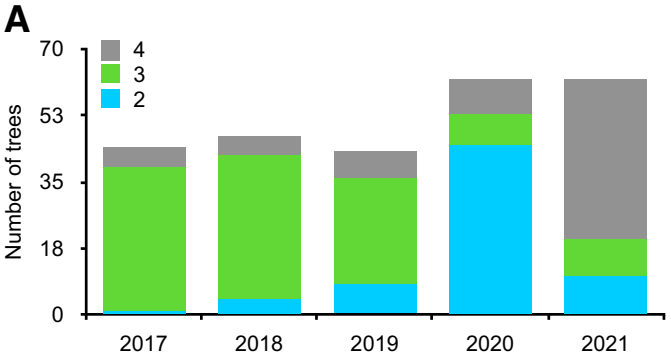

Year	2	3	4	Sum
2017	1	38	5	44
2018	4	38	5	47
2019	8	28	7	43
2020	45	8	9	62
2021	10	10	42	62

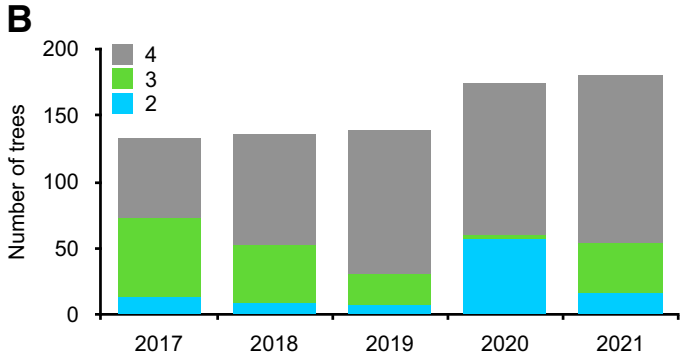

Year	2	3	4	Sum
2017	14	58	60	132
2018	9	43	84	136
2019	8	23	108	139
2020	57	3	114	174
2021	17	37	127	181

Fig. 7. Almond leaf scorch (ALS) dynamics in two orchards in Hula Valley. The number of almond trees showing ALS symptoms with different disease severity ratings in **A,** subplot 1-3 and **B,** subplot 2-1 was recorded and summed for each year from 2017 and 2021 (see detailed maps in Fig. 6). Below the bar graphs are the exact number of trees in each disease rating category every year.

otherwise, we would have expected to see a larger variation in the population. We acknowledge that these conclusions are based on the genome sequence of six isolates and that a larger sample size might have revealed additional insights. The genomic analysis further indicates that the source of *X. fastidiosa* isolates in Israel is from an *X. fastidiosa* subsp. *fastidiosa* population in California. However, it is not yet clear how *X. fastidiosa* was introduced into Israel.

In line with its suspected origin and phylogenetic placement, *X. fastidiosa* isolates from Israel were found to be pathogenic in both almonds and grapevines in mechanical inoculation assays (Almeida and Purcell 2003). These results reveal a possible threat to the wine and table grape industries in Israel, as the pathogen could spread from almonds to grapevines, causing PD. Unsurprisingly, the local *X. fastidiosa* isolates were unable to cause disease symptoms in other crop plants such as olives, citrus, plum, peach, and nectarine, which are known to be infected by other *X. fastidiosa* subspecies. *X. fastidiosa* subsp. *fastidiosa* ST1 was previously isolated from cherry (*P. avium*), suggesting that it can infect this plant species (Olmo et al. 2017). However, in our experiments, we did not observe disease symptoms or significant upward migration of the pathogen from the IP in cherry plants. Unfortunately, we had a limited number of cherry trees for the inoculation assay (eight in total of a single cultivar) and therefore conclude that further testing is required to decidedly determine whether cherry is a host of the local *X. fastidiosa* isolates.

Although not leading to disease symptoms, *X. fastidiosa* was detected by qPCR at the IP of the asymptomatic plant species. Nevertheless, the relative concentration of pathogen cells at the IP was clearly lower than in grapevine and almond and might have already died (Purcell and Saunders 1999). Additionally, *X. fastidiosa* was hardly detected above the IP in the asymptomatic plant species, further supporting the lack of compatibility between the tested *X. fastidiosa* isolates and these crop plants. On the other hand, in almond and grapevine cultivars, *X. fastidiosa* migrated upward from

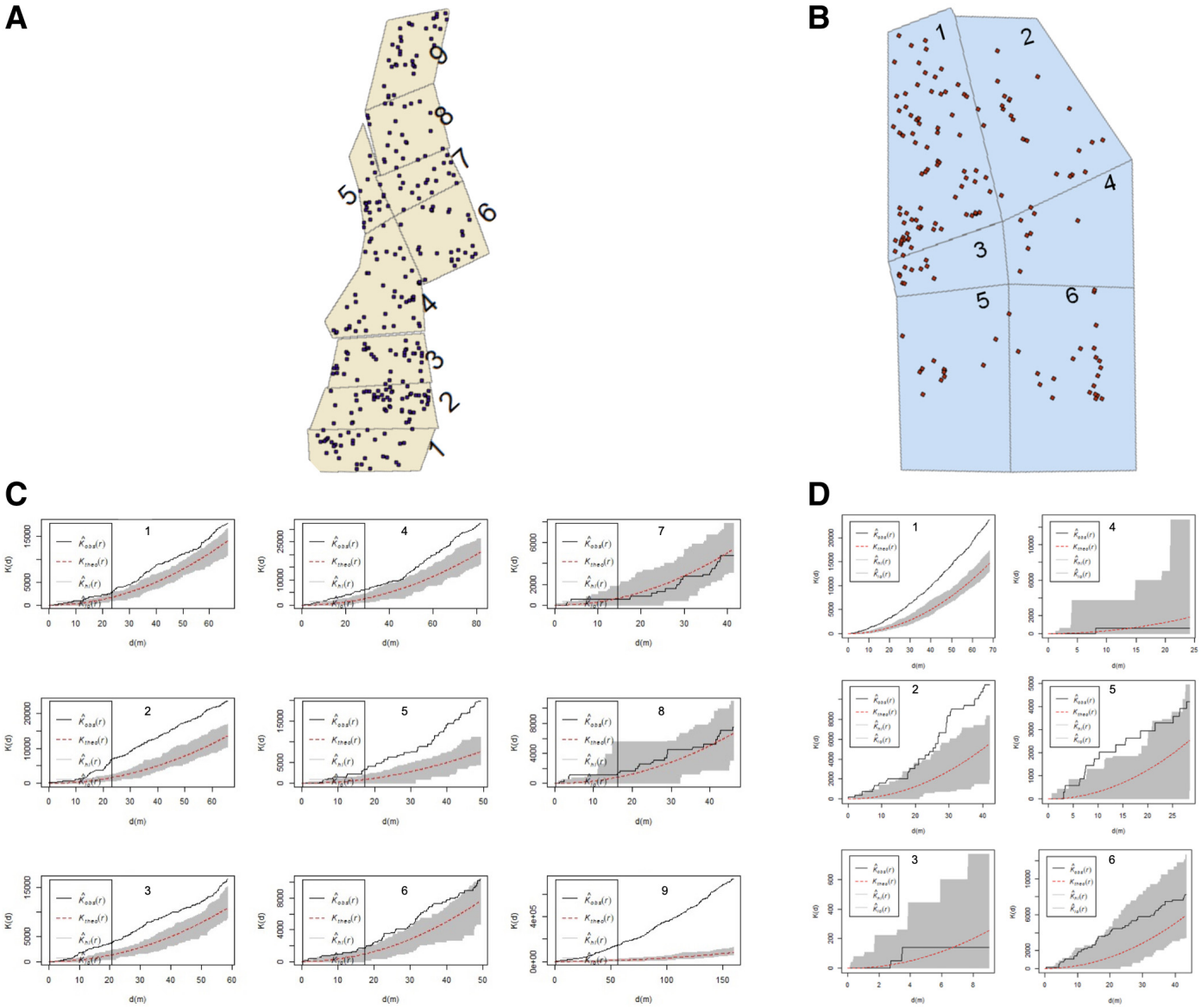

Fig. 8. Spatial analysis of almond leaf scorch (ALS) symptoms in two orchards in Hula Valley. During 2018, each symptomatic tree in **A,** orchard 1 and **B,** orchard 2 was recorded with a GPS-tracking system. Different subplots (denoted by numbers) in each orchard are separated from one another by a gravel road, approximately 4 m in width. Each dot on these maps represents either an ALS symptomatic tree or a dead/uprooted tree. Ripley's K analysis was used to determine the spatial distribution of symptomatic trees in each of the subplots for **C,** orchard 1 and **D,** orchard 2. The estimated K-function (solid black line) and the theoretical K-function (dashed red line) are presented. The gray area denotes the upper and lower limits of a 95% confidence interval of the theoretical K-function (i.e., when the observed K value is larger than the theoretical K value for a particular distance, the distribution is more clustered than a random distribution at that distance). Statistically significant spatial clustering occurs when the estimated K value exceeds the confidence interval value.

the IP (20 cm above or more) in nearly all the inoculated branches. We note that multiple infections per plant were used in this research, as our goal was to assess the potential risks of the local *X. fastidiosa* population to many crops of importance to Israel. Altogether, this indicates that if no further introductions of *X. fastidiosa* into Israel occur, almonds and grapes would be the main crops under threat.

Despite the advanced stage of infection in a substantial number of trees in several orchards in Hula Valley, we did not observe ALS spread in the following 2 years. This, however, changed in 2020 when a clear increase in the number of symptomatic trees was recorded in the two surveyed subplots. Most of the newly identified symptomatic trees in 2020 received a disease severity score of 2, indicating that less than 50% of the canopy was symptomatic. Unexpectedly, most of these trees were asymptomatic in 2021. It is somewhat puzzling how trees that were identified as symptomatic in 2020 were asymptomatic in 2021. Although recovery of infected trees is a possible explanation (Cao et al. 2011; Feil et al. 2003), it seems unlikely that such a large number of trees would recover in the same year in two different orchards. Nevertheless, we cannot rule out this possibility. Another possible explanation is that the symptomatic trees in 2020 were incorrectly designated as such. However, the survey in 2020 was conducted by the same personnel that conducted the surveys in the preceding years and were highly experienced in this task. Perhaps if symptoms are displayed on only a few branches, they might be more difficult to correctly identify, considering that most of the infected trees were severely infected. This could have led to some inconsistencies in symptomatic tree identification in 2020. Nevertheless, in 2021, despite the lack of symptoms in previously symptomatic trees described above, a similar number of symptomatic trees was recorded, some of which received a disease rating of 2. Many of the trees that received a disease severity score of 2 in 2021 were also tested and found to be positive for *X. fastidiosa* (qPCR-based test, data not shown). Overall, the appearance of new symptomatic trees in 2021 supports the presumption that a compatible and active vector, causing secondary spread of ALS, exists in Hula Valley.

The spatial pattern of symptomatic trees within infected almond orchards in Hula Valley was mostly in clusters. It was previously reported that the spatial pattern of ALS depends on the disease incidence levels, where at low incidence, the distribution of infected trees is random, and as incidence increases, infected trees become clustered as a result of vector-mediated secondary infection (Groves et al. 2005). A similar conclusion was obtained by Ferreira et al. (2016), who studied the spatial distribution of plum leaf scald caused by *X. fastidiosa* in Brazil. Hence, our results support the notion that an active insect vector is present in Israel and is responsible for secondary spread of ALS. Our spatial analysis further indicated that the model best describing the disease progression in subplot 2-1 was the model showing spread along the orchard rows. A higher tendency for in-row spread of *X. fastidiosa* was also shown with plum leaf scald and ALS in California (Ferreira et al. 2016; Groves et al. 2005). In the almond orchards we tested, the canopy of adjacent trees in the same row are in physical contact, whereas the canopy of adjacent trees in parallel rows is not. This could indicate that insect vectors are more inclined to move from one tree to another along the row, rather than across rows. In subplot 1-3, in which ALS incidence was lower, the symptoms spread similarly in all directions. These differences between the subplots could stem from the slightly lower disease incidence in subplot 1-3, and it is possible that when incidence in subplot 1-3 increases, a more directional spread of the disease will be seen.

In summary, *X. fastidiosa* subsp. *fastidiosa* was found to be the causal agent of ALS disease in Israel. Our surveys in the past 5 years revealed that there is little spread of ALS within orchards, based on appearance of symptomatic trees. This could be a result of low abundance and/or efficiency of local *X. fastidiosa* vectors, which have yet to be identified. Nevertheless, the possible transmission of *X. fastidiosa* to grapevines and infliction of PD, along with potential changes in vector species, population size, and behavior, could lead to a more significant outbreak in the future and should therefore be considered as a threat to both the almond and viticulture industries in Israel.

Acknowledgments

We thank the growers of orchard 1 and orchard 2 and the PPIS monitoring and ecology team for their valuable collaboration throughout this study. We thank the Newe Yaar Research Center for providing almond seedlings for inoculation experiments.

Literature Cited

Almeida, R. P. P., and Purcell, A. H. 2003. Biological traits of *Xylella fastidiosa* strains from grapes and almonds. Appl. Environ. Microbiol. 69:7447-7452.

Amanifar, N., Taghavi, M., Izadpanah, K., and Babaei, G. 2009. Isolation and pathogenicity of *Xylella fastidiosa* from grapevine and almond in Iran. Phytopathol. Mediterr. 53:318-327.

Andrews, S., Wingett, S. W., and Hamilton, R. S. 2018. FastQ Screen: A tool for multi-genome mapping and quality control. F10000Res 7:1328.

Baddeley, A., Rubak, E., and Turner, R. 2015. Spatial Point Patterns: Methodology and Applications with R. Chapman & Hall/CRC Press, London, U.K.

Bankevich, A. 2012. SPAdes: A new genome assembly algorithm and its applications to single-cell sequencing. J. Comput. Biol. 19:455-477.

Ben-Hamo, M., Ezra, D., Krasnov, H., and Blank, L. 2020. Spatial and temporal dynamics of Mal Secco disease spread in lemon orchards in Israel. Phytopathology 110:863-872.

Bragard, C., Dehnen-Schmutz, K., Di Serio, F., Gonthier, P., Jacques, M.-A., Miret, J. A. J., Justesen, A. F., MacLeod, A., Magnusson, C. S., Milonas, P., Navas-Cortés, J. A., Parnell, S., Potting, R., Reignault, P. L., Thulke, H.-H., Van der Werf, W., Civera, A. V., Yuen, J., and Zappalà, L. 2019. Update of the scientific opinion on the risks to plant health posed by *Xylella fastidiosa* in the EU territory. EFSA J. 17:5655.

Cao, T., Connell, J. H., Wilhelm, M., and Kirkpatrick, B. C. 2011. Influence of inoculation date on the colonization of *Xylella fastidiosa* and the persistence of almond leaf scorch disease among almond cultivars. Plant Dis. 95: 158-165.

Castillo, A. I., Bojanini, I., Chen, H., Kandel, P. P., De La Fuente, L., and Almeida, R. P. P. 2021. Allopatric plant pathogen population divergence following disease emergence. Appl. Environ. Microbiol. 87:1-19.

Castillo, A. I., Chacón-Díaz, C., Rodríguez-Murillo, N., Coletta-Filho, H. D., and Almeida, R. P. P. 2020. Impacts of local population history and ecology on the evolution of a globally dispersed pathogen. BMC Genom. 21:369.

Chang, C. J., Garnier, M., Zreik, L., Rossetti, V., and Bové, J. M. 1993. Culture and serological detection of the xylem-limited bacterium causing citrus variegated chlorosis and its identification as a strain of *Xylella fastidiosa*. Curr. Microbiol. 27:137-142.

Cornara, D., Cavalieri, V., Dongiovanni, C., Altamura, G., Palmisano, F., Bosco, D., Porcelli, F., Almeida, R. P. P., and Saponari, M. 2017. Transmission of *Xylella fastidiosa* by naturally infected *Philaenus spumarius* (Hemiptera, Aphrophoridae) to different host plants. J. Appl. Entomol. 141: 80-87.

Cornara, D., Saponari, M., Zeilinger, A. R., de Stradis, A., Boscia, D., Loconsole, G., Bosco, D., Martelli, G. P., Almeida, R. P. P., and Porcelli, F. 2016. Spittlebugs as vectors of *Xylella fastidiosa* in olive orchards in Italy. J. Pest Sci. 90:521-530.

Davis, M. J., French, W. J., and Schaad, N. W. 1981. Axenic culture of the bacteria associated with phony disease of peach and plum leaf scald. Curr. Microbiol. 6:309-314.

Davis, M. J., Thomson, S., and Purcell, A. H. 1980. Etiological role of the xylem-limited bacterium causing Pierce's disease in almond leaf scorch. Phytopathology 70:472.

Delbianco, A., Gibin, D., Pasinato, L., and Morelli, M. 2021. Update of the *Xylella* spp. host plant database–Systematic literature search up to 31 December 2020. EFSA J. 19:e06674.

Denancé, N., Legendre, B., Briand, M., Olivier, V., de Boisseson, C., Poliakoff, F., and Jacques, M.-A. 2017. Several subspecies and sequence types are associated with the emergence of *Xylella fastidiosa* in natural settings in France. Plant Pathol. 66:1054-1064.

EFSA PLH Panel (EFSA Panel on Plant Health), Jeger, M., Caffier, D., Candresse, T., Chatzivassiliou, E., Dehnen-Schmutz, K., Gilioli, G., Gregoire, J. C., Jaques Miret, J. A., MacLeod, A., Navajas Navarro, M., Niere, B., Parnell, S., Potting, R., Rafoss, T., Rossi, V., Urek, G., Van Bruggen, A., Van der Werf, W., West, J., Winter, S., Almeida, R., Bosco, D., Jacques, M. A., Landa, B., Purcell, A., Saponari, M., Czwienczek, E., Delbianco, A., Stancanelli, G., and Bragard, C. 2018. Scientific opinion on the updated pest categorisation of *Xylella fastidiosa*. EFSA J. 16:5357.

EFSA Panel on Plant Health. 2015. Scientific opinion on the risk to plant health posed by *Xylella fastidiosa* in the EU territory, with the identification and evaluation of risk reduction options. EFSA J. 13:3989.

Feil, H., Feil, W. S., and Purcell, A. H. 2003. Effects of date of inoculation on the within-plant movement of *Xylella fastidiosa* and persistence of Pierce's disease within field grapevines. Phytopathology 93:244-251.

Ferreira, G. M., Mascaro, F. D. A., Dalla Pria, M., Ribeiro Junior, P. J., and De Mio, L. L. M. 2016. Spatial analysis of plum leaf scald in São Paulo State, Brazil. J. Plant Pathol. 98:511-518.

Giampetruzzi, A., Velasco-amo, P., Marco-noales, E., Montes-borrego, M., Navarro, I., Monterde, A., Barbé, S., Almeida, R. P. P., Saldarelli, P., Saponari, M., Montilon, V., Savino, V. N., Boscia, D., and Landa, B. B. 2019. Draft genome resources of two strains ("ESVL" and "IVIA5901") of *Xylella fastidiosa* associated with almond leaf scorch disease in Alicante, Spain. Phytopathology 109:219-221.

Groves, R. L., Chen, J., Civerolo, E. L., Freeman, M. W., and Viveros, M. A. 2005. Spatial analysis of almond leaf scorch disease in the San Joaquin Valley of California: Factors affecting pathogen distribution and spread. Plant Dis. 89:581-589.

Harper, S. J., Ward, L. I., and Clover, G. R. G. 2010. Development of LAMP and real-time PCR methods for the rapid detection of *Xylella fastidiosa* for quarantine and field applications. Phytopathology 100:1282-1288.

Hill, B. L., and Purcell, A. H. 1997. Populations of *Xylella fastidiosa* in plants required for transmission by an efficient vector. Phytopathology 87: 1197-1201.

Hopkins, D. L. 1989. *Xylella fastidiosa*: Xylem-limited bacterial pathogen of plants. Annu. Rev. Phytopathol. 27:271-290.

Jacques, M.-A., Denancé, N., Legendre, B., Morel, E., Briand, M., Mississipi, S., Durand, K., Olivier, V., Portier, P., Poliakoff, F., and Crouzillat, D. 2016. New coffee plant-infecting *Xylella fastidiosa* variants derived via homologous recombination. Appl. Environ. Microbiol. 82:1556-1568.

Janse, J. D., and Obradovic, A. 2010. *Xylella fastidiosa*: Its biology, diagnosis, control and risks. J. Plant Pathol. 92:S35-S48.

Katoh, K., and Standley, D. M. 2013. MAFFT: Multiple sequence alignment software version 7: Improvements in performance and usability. Mol. Biol. Evol. 30:772-780.

Landa, B. B., Castillo, A. I., Giampetruzzi, A., Kahn, A., Román-Écija, M., Velasco-Amo, M. P., Navas-Cortés, J. A., Marco-Noales, E., Barbé, S., Moralejo, E., Coletta-Filho, H. D., Saldarelli, P., Saponari, M., and Almeida, R. P. P. 2020. Emergence of a plant pathogen in Europe associated with multiple intercontinental introductions. Appl. Environ. Microbiol. 86: e01521-19.

Langmead, B., and Salzberg, S. L. 2012. Fast gapped-read alignment with Bowtie 2. Nat. Methods 9:357-359.

Leu, L. S., and Su, C. C. 1993. Isolation, cultivation, and pathogenicity of *Xylella fastidiosa*, the causal bacterium of pear leaf scorch disease in Taiwan. Plant Dis. 77:642-646.

Li, H., Handsaker, B., Wysoker, A., Fennell, T., Ruan, J., Homer, N., Marth, G., Abecasis, G., and Durbin, R., and 1000 Genome Project Data Processing Subgroup. 2009. The sequence alignment /map format and SAMtools. Bioinformatics 25:2078-2079.

Loconsole, G., Saponari, M., Boscia, D., D'Attoma, G., Morelli, M., Martelli, G. P., and Almeida, R. P. P. 2016. Intercepted isolates of *Xylella fastidiosa* in Europe reveal novel genetic diversity. Eur. J. Plant Pathol. 146: 85-94.

Marcel, M. 2011. Cutadapt removes adapter sequences from high-throughput sequencing reads. EMBnet J. 17:5-7.

Martelli, G. P., Boscia, D., Porcelli, F., and Saponari, M. 2015. The olive quick decline syndrome in south-east Italy: A threatening phytosanitary emergency. Eur. J. Plant Pathol. 144:235-243.

Mawassi, M., Dror, O., Bar-Joseph, M., Piasetzky, A., Sjölund, J., Levitzky, N., Shoshana, N., Meslenin, L., Haviv, S., Porat, C., Katsir, L., Svetlana, K., Ghanim, M., Zelinge-Reichert, E., Arnsdorf, M. Y., Gera, A., and Bahar, O. 2018. '*Candidatus* Liberibacter solanacearum' is tightly associated with carrot yellows symptoms in Israel and transmitted by the prevalent psyllid vector *Bactericera trigonica*. Phytopathology 108:1056-1066.

Minsavage, G., Thompson, C., Hopkins, D., Leite, R., and Stall, R. 1994. Development of a polymerase chain reaction protocol for detection of *Xylella fastidiosa* in plant tissue. Phytopathology 84:456-461.

Moralejo, E., Borràs, D., Gomila, M., Montesinos, M., Adrover, F., Juan, A., Nieto, A., Olmo, D., Seguí, G., and Landa, B. B. 2019. Insights into the epidemiology of Pierce's disease in vineyards of Mallorca. Spain. Plant Pathol. 68:1458-1471.

Moralejo, E., Gomila, M., Montesinos, M., Borràs, D., Pascual, A., Nieto, A., Adrover, F., Gost, P. A., Seguí, G., Busquets, A., Jurado-Rivera, J. A., Quetglas, B., de Dios García, J., Beidas, O., Juan, A., Velasco-Amo, M. P., Landa, B. B., and Olmo, D. 2020. Phylogenetic inference enables reconstruction of a long-overlooked outbreak of almond leaf scorch disease (*Xylella fastidiosa*) in Europe. Commun. Biol. 3:1-13A.

Mostowy, R., Croucher, N. J., Andam, C. P., Corander, J., Hanage, W. P., and Marttinen, P. 2017. Efficient inference of recent and ancestral recombination within bacterial populations. Mol. Biol. Evol. 34: 1167-1182.

Nunney, L., Ortiz, B., Russell, S. A., Ruiz Sánchez, R., and Stouthamer, R. 2014a. The complex biogeography of the plant pathogen *Xylella fastidiosa*: Genetic evidence of introductions and subspecific introgression in Central America. PLoS One 9:e112463.

Nunney, L., Schuenzel, E. L., Scally, M., Bromley, R. E., and Stouthamerc, R. 2014b. Large-scale intersubspecific recombination in the plant-pathogenic bacterium *Xylella fastidiosa* is associated with the host shift to mulberry. Appl. Environ. Microbiol. 80:3025-3033.

Nunney, L., Yuan, X., Bromley, R. E., and Stouthamer, R. 2012. Detecting genetic introgression: High levels of intersubspecific recombination found in *Xylella fastidiosa* in Brazil. Appl. Environ. Microbiol. 78: 4702-4714.

Nurk, S., Bankevich, A., Antipov, D., Gurevich, A., Korobeynikov, A., Lapidus, A., Prjibelski, A., Pyshkin, A., Sirotkin, A., Sirotkin, Y., Stepanauskas, R., Clingenpeel, S., Woyke, T., McLean, J., Lasken, R., Tesler, G., and Alekseyev, M. P. 2013. Assembly single-cell genomes and mini-metagenomes from chimeric MDA products. J. Comput. Biol. 20:714-737.

Olmo, D., Nieto, A., Adrover, F., Urbano, A., Beidas, O., Juan, A., Marco-Noales, E., López, M. M., Navarro, I., Monterde, A., Montes-Borrego, M., Navas-Cortés, J. A., and Landa, B. B. 2017. First detection of *Xylella fastidiosa* infecting cherry (*Prunus avium*) and *Polygala myrtifolia* plants, in Mallorca Island, Spain. Plant Dis. 101:1820.

Page, A. J., Cummins, C. A., Hunt, M., Wong, V. K., Reuter, S., Holden, M. T. G., Fookes, M., Falush, D., Keane, J. A., and Parkhill, J. 2015. Roary: Rapid large-scale prokaryote pan genome analysis. Bioinformatics 31: 3691-3693.

Pfeifer, B., Wittelsbu, U., Ramos-onsins, S. E., and Lercher, M. J. 2014. PopGenome : An efficient Swiss army knife for population genomic analyses in R. Mol. Biol. Evol. 31:1929-1936.

Pierce, N. B. 1892. The California Vine Disease. Division of Vegetable Pathology, U.S. Department of Agriculture. Bulletin No. 2:215.

Purcell, A. H., and Finlay, A. 1979. Evidence for noncirculative transmission of Pierce's disease bacterium by sharpshooter leafhoppers. Phytopathology 69:393-395.

Purcell, A. H., and Hopkins, D. L. 2002. Fastidious xylem-limited bacterial plant pathogens. Annu. Rev. Phytopathol. 34:131-151.

Purcell, A. H., and Saunders, S. R. 1999. Fate of Pierce's disease strains of *Xylella fastidiosa* in common riparian plants in California. Plant Dis. 83: 825-830.

Purcell, A. H., Saunders, S. R., Hendson, M., Grebus, M. E., and Henry, M. J. 1999. Causal role of *Xylella fastidiosa* in Oleander leaf scorch disease. Phytopathology 89:53-58.

Quinlan, A. R., and Hall, I. M. 2010. BEDTools: A flexible suite of utilities for comparing genomic features. Bioinformatics 26:841-842.

Ripley, B. D. 1976. The second order analysis of stationary point processes. J. Appl. Probab. 13:255-266.

Rissman, A. I., Mau, B., Biehl, B. S., Darling, A. E., Glasner, J. D., and Perna, N. T. 2009. Reordering contigs of draft genomes using the Mauve aligner. Bioinformatics 25:2071-2073.

Sanborn, R. R., Mircetich, S. M., Nyland, G., and Moller, W. J. 1974. "Golden death": A new leaf scorch threat to almond growers. Hilgardia 28:4-5.

Saponari, M., Boscia, D., Altamura, G., Loconsole, G., Zicca, S., D'Attoma, G., Morelli, M., Palmisano, F., Saponari, A., Tavano, D., Savino, V. N., Dongiovanni, C., and Martelli, G. P. 2017. Isolation and pathogenicity of *Xylella fastidiosa* associated to the olive quick decline syndrome in southern Italy. Sci. Rep. 7:17723.

Saponari, M., Boscia, D., Nigro, F., and Martelli, G. P. 2013. Identification of DNA sequences related to *Xylella fastidiosa* in oleander, almond and olive trees exhibiting leaf scorch symptoms in Apulia (Southern Italy). J. Plant Pathol. 95:668.

Saponari, M., Giampetruzzi, A., Loconsole, G., Boscia, D., Saldarelli, P., and Amendola, A. 2019. *Xylella fastidiosa* in olive in Apulia: Where we stand. Phytopathology 109:175-186.

Scally, M., Schuenzel, E. L., Stouthamer, R., and Nunney, L. 2005. Multilocus sequence type system for the Plant Pathogen *Xylella fastidiosa* and relative contributions of recombination and point mutation to clonal diversity. Appl. Environ. Microbiol. 71:8491-8499.

Schneider, K., van der Werf, W., Cendoya, M., Mourits, M., Navas-Cortés, J. A., Vicent, A., and Lansink, O. A. 2020. Impact of *Xylella fastidiosa* subspecies *pauca* in European olives. Proc. Natl. Acad. Sci. U.S.A. 117: 9250-9259.

Seemann, T. 2014. Prokka: Rapid prokaryotic genome annotation. Bioinformatics 30:2068-2069.

Sicard, A., Saponari, M., Vanhove, M., Castillo, A. I., Giampetruzzi, A., Loconsole, G., Saldarelli, P., Boscia, D., Neema, C., and Almeida, R. P. P.

2021. Introduction and adaptation of an emerging pathogen to olive trees in Italy. Microbiol. Genomics 7:000735.

Sicard, A., Zeilinger, A. R., Vanhove, M., Schartel, T. E., Beal, D. J., Daugherty, M. P., and Almeida, R. P. P. 2018. *Xylella fastidiosa*: Insights into an emerging plant pathogen. Annu. Rev. Phytopathol. 56:181-202.

Soubeyrand, S., de Jerphanion, P., Martin, O., Saussac, M., Manceau, C., Hendrikx, P., and Lannou, C. 2018. Inferring pathogen dynamics from temporal count data: The emergence of *Xylella fastidiosa* in France is probably not recent. New Phytol. 219:824-836.

Sparks, A. H., Esker, P. D., Antony, G., Campbell, L., Frank, E. E., Huebel, L., Rouse, M. N., Van Allen, B., and Garrett, K. A. 2008. Ecology and epidemiology in R: Spatial pattern analysis. Plant Health Instr. https://doi.org/10.1094/PHI-A-2008-0129-04

Stamatakis, A. 2014. RAxML version 8: A tool for phylogenetic analysis and post-analysis of large phylogenies. Bioinformatics 30:1312-1313.

Su, C. C., Chang, C. J., Chang, C. M., Shih, H. T., Tzeng, K. C., Jan, F. J., Kao, C. W., and Deng, W. L. 2013. Pierce's disease of grapevines in Taiwan: Isolation, cultivation and pathogenicity of *Xylella fastidiosa*. J. Phytopathol. 161:389-396.

Sun, Q., Sun, Y., Walker, M. A., and Labavitch, J. M. 2013. Vascular occlusions in grapevines with Pierce's disease make disease symptom development worse. Plant Physiol. 161:1529-1541.

Tajima, F. 1989. Statistical method for testing the neutral mutation hypothesis by DNA polymorphism. Genet. Soc. Am. 595:585-595.

Tumber, K. P., Alston, J. M., and Fuller, K. B. 2014. Pierce's disease costs California $104 million per year. Calif. Agric. 68:20-29.

Vanhove, M., Sicard, A., Ezennia, J., Leviten, N., and Almeida, R. P. P. 2020. Population structure and adaptation of a bacterial pathogen in California grapevines. Environ. Microbiol. 22:2625-2638.

Watterson, G. A. 1975. On the number of segregating sites in genetical models without recombination. Theor. Popul. Biol. 7:256-276.

Zhang, Y. P., Uyemoto, J. K., and Kirkpatrick, B. C. 1998. A small-scale procedure for extracting nucleic acids from woody plants infected with various phytopathogens for PCR assay. J. Virol. Methods 71:45-50.